A method to employ the spatial organisation of catchments into semi-distributed rainfall-runoff models

Henning Oppel[1], Andreas Schumann[1]

[1]Institute of Hydrology, Water Resources Management and Environmental Engineering, Ruhr-University Bochum, Bochum, 44801, Germany

Correspondence to: Henning Oppel (henning.oppel@rub.de)

Abstract.

A distributed or semi-distributed deterministic hydrological model should consider the hydrological most relevant catchment characteristics. These are heterogeneously distributed within a watershed but often interrelated and subject of a certain spatial organisation which results in archetypes of combined characteristics. In order to reproduce the natural rainfall-runoff response the reduction of variance of catchment properties as well as the incorporation of the spatial organisation of the catchment is desirable. In this study the width-function approach is utilized as a basic characteristic to analyse the succession of catchment characteristics. By applying this technique we were able to assess the context of catchment properties like soil or topology along the stream flow length and the network geomorphology, giving indications on the spatial organisation of a catchment. Moreover, this information and technique have been implemented in an algorithm for automated sub-basin ascertainment, which included the definition of zones within the newly defined sub-basins. The objective was to provide sub-basins that were less heterogeneous than common separation schemes. The algorithm was applied on two parameters characterising topology and soil of four mid-European watersheds. Resulting partitions indicated a wide range of applicability for the method and the algorithm. Additionally, the intersection of derived zones for different catchment characteristics could give insights on sub-basin similarities. Finally, a HBV_{96}-case study demonstrated the potential benefits of modelling with the new subdivision technique.

1 Introduction

Hydrological models are instruments for structuring the knowledge of hydrological processes in their dependence on watershed characteristics. For the set-up of these models several initial decisions have to be made, e.g.:

- Which type of model has to be used?
- Which temporal resolution could be appropriate?
- Which spatial resolution of the model would be necessary and useful?
- Which way could the model be parameterised?

It is obvious that all of these options will affect the effort of the model and all choices have to consider the modelling purpose. Furthermore, these choices are interrelated, for example predominant soil properties define the dominant runoff process and should, hence, define the used model. Therefore, conceptual models of a natural watershed require its subdivision into spatial units which should be as homogeneous as possible. Hydrological modelling is the attempt to specify hydrological processes quantitatively under consideration of boundary conditions. These boundary conditions are mainly determined by spatial heterogeneously distributed catchment characteristics. There are several approaches to address this heterogeneity in models to enable working with more or less homogeneous units.

One option to address spatial heterogeneity might be the subdivision of a river basin into sub-basins which have to be modelled separately. The common approach for such a subdivision is usually based on available hydro-meteorological data, though the correct criteria would be the spatial heterogeneity of hydrological characteristics within the river basin. If the heterogeneity is at a low level, neighbouring basins could be modelled in accordance. In the reverse case, i.e. at a high level of heterogeneity, sub-basins should be modelled separately with an especially adapted model taking into account their specific characteristics (e.g. an urban watershed model). Subsequently each sub-basin needs to be treated as a unique modelling instance that should provide a minimum level of heterogeneity (regarding key catchment characteristic). This way each sub-basin would end up with its own unique model and/or parameter set to adjust the model to mimic its natural response.

Another option to address spatial heterogeneity within a watershed could be splitting the catchment into so-called hydrologic response units (HRUs). A single unit merges areas, or cells, within a basin displaying similar characteristics independent from their respective spatial allocation, i.e. each unit is a unique modelling instance. The HRU approach is based on the key assumption that the variation of the hydrological process dynamics within the HRU must be low relative to the dynamics in another HRU (Flügel, 1995). HRUs are developed by intersecting different data layers of different physiographic criteria. The delineation of HRUs by combinations of these layers requires a categorisation of its characteristics (soils, land-use and vegetation types, topography, and geology) to keep the number of HRUs at a manageable level. Both, the selection of criteria and their subdivision into classes at an acceptable degree of heterogeneity within the hydrological system. Subject to the chosen technique or purpose of HRUs, their models omit the actual spatial allocation (Lindström et al., 1997; Schumann et al., 2000) or define coherent units (Dunn and Lilly, 2001; Soulsby et al., 2006; Müller et al., 2009; Nobre et al., 2011; Gharari et al., 2011). However, some of these models try to transfer geological information (Müller et al., 2009; Soulsby et al., 2006) or topographical information (Nobre et al., 2011; Gharari et al., 2011) to hydrological processes and assume homogeneous conditions of remaining parameters.

A third option to address spatial heterogeneity in hydrological modelling is the utilisation of a distributed catchment characteristic as a covariant metric supporting the spatial distribution of a lumped state variable. An example for this approach is the use of the topographic index in the well-known TOP-model as a characteristic of the spatial variability of the soil water content (Beven et al., 1984).

Since GIS layers are widely available, there is an obvious trend to incorporate this data into the ascertainment of spatial units. Most approaches are based on topography (Band, 1986; Moore and Grayson, 1991; Vogt et al., 2003; Lai et al., 2016) and focus on the extraction of stream networks and the network connectivity, utilizing topology driven modelling concepts (Beven and Kirkby, 1979; Rodríguez-Iturbe and Valdés, 1979). Particularly the development of the geomorphologic instantaneous unit hydrograph (GIUH) as well as its enhancements like the geomorphological dispersion (Rinaldo et al., 1991; Gupta and Mesa, 1988)require sophisticated stream network derivation and analysis. Methods introduced by Band (1986) or Verdin and Verdin (1999) were developed to generate data to meet this requirement. Furthermore Snell and Sivapalan (1994) applied the width-function, introduced by Kirkby (1976), to model the geomorphic structure of networks. Snell and Sivapalan (1994) were able to demonstrate that GIUHs based on the width function provide a better geomorphic dispersion than GUIHs derived from Horton laws (Robinson et al., 1995; D'Odorico and Rigon, 2003; Rigon et al., 2016). This has been a further step to incorporate remote sensed data in describing the organisation of catchments. While above described methods are based on gridded digital elevation models (DEM) other methods try to identify streamlines derived from DEM-shapes, producing contour-lines (Moore and Grayson, 1991; Lai et al., 2016) that are subsequently used as modelling instances.

The following sections of this paper will present a combination of different methods to address spatial heterogeneity of watershed characteristics, utilizing patterns resulting from the spatial organisation of catchments. Sivapalan (2005) pointed out that the organisation of a catchment has a fundamental influence on the hydrological system. He defined the organisation of a catchment as patterns of symmetry between soil, topography and the stream network. These patterns could unveil underlying mechanisms that induce discharge behaviour. Combining soil data with the flow path lengths at hillslopes in particular could provide a better understanding of lateral flow distribution processes (Grayson and Blöschl, 2001).

In this study we will present a method to address these patterns by combining the width-function (Kirkby, 1976; Mesa and Mifflin, 1986) with soil properties like pore volume and topographic characteristics like surface slope. Unlike traditional methods for spatial pattern evaluation (like Point-by-Point or optimal logical alignment methods (Grayson and Blöschl, 2001)) we retain the allocation of catchment properties. This analysis revealed the organisation of the watershed and gave indications of spatial heterogeneity gradations which could be useful for the set-up of an appropriated model structure.

Applying this method we developed an algorithm for automated sub-basin ascertainment. Our objective was to incorporate the spatial organisation of watersheds into the spatial structuring of a semi-distributed model and to assess its benefits for model performance. The purpose of the proposed algorithm was to provide a basin partition with a minimum of heterogeneity by a minimum of sub-divisions, i.e. to reduce the number of unnecessary sub-divisions and subsequently the number of parameters in cases of hydrological modelling.

The proposed algorithm has been applied in a case study to four meso-scale mid-European watersheds and in a HBV_{96} modelling application in one of these basins. Remaining heterogeneity and the modelling performance of the proposed subdivision scheme were compared to a common subdivision / modelling setup.

The presentation has been split into four sections:

- Data, giving references to observations in some of the basins during the description of the methodological development.
- Methodological development, including observations, considerations and techniques to assess spatial patterns of catchment characteristics and their spatial organisation. In this section the sequence of the proposed algorithms will be presented which was utilized to incorporate the spatial organisations into the model.
- Method analysis i.e. checking their applicability and their limits.
- Method application, including the subdivision case study and modelling application.

2 Data

Due to the fact that the proposed methods were based on GIS-based catchment analysis, we first had to establish our data base first. In general, four catchments were selected to develop and test our methodological approach with one catchment serving as a development catchment and the remaining catchments for validation. Our development catchment was the Mulde River basin (Fig. 1, left). The basin is actually located mainly in Eastern Germany with a small section in Northern Czech. Its southern section is located in the mid-range mountainous region of the Ore Mountains. With a size of 6170 km^2 it is the largest catchment used in this study. The three other catchments are the catchments of the rivers Regen (A = 2613 km^2, Fig. 1, lower mid), upper Main (A = 4224 km2, Fig. 1, upper mid) and Salzach (A = 5995 km^2, Fig 1, right). While the Mulde, Main and Regen basins are mid-mountainous catchments the Salzach basin is an alpine catchment. All catchments have different geomorphologic structures and river network types. While in the first three catchments, higher mountains are nearly exclusively located at the outer catchment boundaries, the Salzach catchment contains three high mountains located in the centre of the catchment. The two main tributaries encompass these mountains. While the Mulde River basin has a nearly continuous increase of slope and elevation from north to south, the topography of the remaining catchments is much more heterogeneous.

A digital elevation model (DEM) is essential for the proposed methods and the algorithm. We used a gridded DEM derived from the Shuttle Radar Topography Mission (SRTM) with a regular resolution of 100 meters. By application of the D8-algorithm the required data, i.e. flow directions, flow length and flow accumulation (i.e. number of cells draining to the respective cell) were calculated (Jenson and Domingue, 1988). For the catchment of the Mulde River a proved digital river network was already available. Stream networks of the remaining basins were calculated via flow accumulation algorithms. To characterise the soil characteristics of the German catchments, a gridded soil data map from the German Federal Institute for Geosciences and Natural Resources (BÜK200) and CORINE land coverage data (CLC) (Bossard et al., 2000) were used. Pedo-transfer functions (Sponagel, 2005) were applied to transfer this information into gridded data of (available) water capacities (AWC), maximum soil storage capacity (referred as total pore volume TPV) and hydraulic conductivity (HC) for

the upper soil, up to two meters depth. In case of the Salzach basin precast pore volume data provided for Europe along with the LARSIM-ME model were used, due to a lack of soil data (Bremicker, 2016). The used soil and topography input data unfortunately include a certain level of uncertainty because these were derived data. However, this was assessed to be negligible for the performed case studies. The pore volume (TPV) data were summarized in Fig. 2.

3 Methodological development

This section introduces an algorithm that characterises the heterogeneity of regions and applies techniques to efficiently subdivide the watershed. In order to make the sequence of the algorithm easier to understand we will first introduce all required new techniques and methods and then present the algorithm.

First, the underlying approach of the distance-factor function for the assessment of spatial organisations (Sec. 3.1) will be presented. Next the tools of the algorithm (Sec. 3.2) will be introduced followed by Sec. 3.3 presenting the sequence of the proposed algorithm. All tools are only introduced briefly, a detailed description of the applied methodologies can be found in the Appendix.

3.1 Distance-factor function

Throughout the development and ongoing research of the geomorphologic instantaneous unit hydrograph (Rodríguez-Iturbe and Valdés, 1979; Gupta et al., 1980) the width-function as introduced by (Kirkby, 1976) and the subsequently developed area- or weight-function (Mesa and Mifflin, 1986; Snell and Sivapalan, 1994; Robinson et al., 1995) were applied to describe the distribution of runoff producing area with respect to flow distance from the outlet (Mesa and Mifflin, 1986). In particular the weight-function provided the probability distribution for a uniform areal precipitation intensity for the choice of a flow path (Snell and Sivapalan, 1994). Since the the flow path and distance is known, we can describe the hydrograph at the outlet of a basin under the assumption of a uniform velocity.

However, velocity in reality is not uniform in a basin. It is subject to its surrounding medium (soil, air, other water particles) and the medium condition (dry or wet/empty or full) and a wide range of other impact factors. We would describe the transformation from the arrival of precipitation at its flow path to the outlet of the catchment as the trail-function. It merges losses and retention of water along the flow path. The detailed description of the trail-function is part of a hydrological model which at this point, is open to the deliberate choice of the user.

In general nearly all hydrological models require information about catchment characteristic(s) or at least homogeneous conditions of a single characteristic (in most cases soil properties). Coming back to the idea of the weight-function, it seemed worthwhile to develop a method to assess an arbitrary catchment characteristic in the same manner.

We propose the *distance-factor function* for analysing the distribution of an arbitrary catchment property C for the flow path. To do so we split the flow path into the section going through (or along) the hillslope (hillslope flow length x_H) and the section streaming to the outlet (stream flow length x_S). It has to be noted that stream cells have a hillslope flow length of 0

and hillslope cells comprise of the x_S of their draining stream cell. Furthermore it has to kept in mind that the term flow length refers to the actual length of the path water has to travel to the outlet, its calculation being based on the D8-algorithm (Jenson and Domingue, 1988).

To assess groups of hillslopes and to account for the non-continuousness of grid-based distances we substituted the estimated flow lengths (x_S and x_H) by distance classes. The stream flow length was subdivided into multiples of the length Δs (for x_S) and the hillslope flow length subdivided into multiples of the distances Δo (for x_H). Distance classes defined in this way will split the basin into stripes. Depending on the width Δs the basin would be classified into N_S distance classes, where N_S is an integer larger or equal to one.

Let us now look at a single distance class *i*, where *i* indicates the class. All cells of the input data with a flow distance in a range between $i \cdot \Delta s$ and $(i+1) \cdot \Delta s$ are assigned to this distance class. We can write the set of distances of x_S assigned to *i* as the following set *B*:

$$B = \left[i \cdot \Delta s; (i+1) \cdot \Delta s \right] \tag{1}$$

To characterise a property C in the distance class *i* we can calculate the expected value *E(C)* and standard deviation $\sigma(C)$, taking only those values of C into account that are situated in the boundaries of the distance classes:

$$E(C)_i = \frac{1}{w(i \cdot \Delta s)} \sum_{(j | x_{s;j} \in B)} C_j \qquad (2) \quad \text{and} \qquad \sigma(C)_i = \sqrt{\frac{1}{w(i \cdot \Delta s)} \sum_{(j | x_{s;j} \in B)} \left(C_j - E(C)_i \right)^2}, \qquad (3)$$

where $w(i \cdot \Delta s)$ represents the number of values (or grid cells) within the class. Please note that w(x) is the non-normalised value of the area-function (Snell and Sivapalan, 1994). To visualise the proposed function a simple synthetic basin with its stream network, distance-classes and an arbitrary characteristic is shown in Fig. 3. To keep things simple Fig. 3c shows the unified flow length (comprising x_S and x_H) derived from the flow direction data in Fig. 3b. As it can be seen in Fig. 3c the basin has been split into 5 distance classes. Applying Eq. 1 and 2 to the data (Fig. 3a) produces the average and standard deviation within these five distance classes. The obtained distance-factor function is shown in Fig. 4.

Figure 5 shows the application to real data in a meso-scale catchment, namely for AWC in the Mulde catchment. Expected values and a 1-σ-range were plotted against the stream flow distance to the outlet. Distance classes with lower and higher variance are clearly visible in this figure as well as the succession of lower values to higher expected AWC values with increasing stream flow lengths.

Taking this approach we will be able to assess the arrangement of catchment properties with the flow-path which will, in case of a non-random arrangement, be referred to as the spatial organisation of the basin. Please note that we will always co-notate which type of distance-factor function (expected value or standard deviation) has been applied.

3.2 Tools for automated sub-basin ascertainment

The example of a distance-factor function in Fig. 5 shows that in some distance classes the AWC-values are at a similar level due to a low standard deviation. This could be caused by the small size of the distance class (which is the case close to the outlet and in the furthest distance class) but also by the fact that the class is located in the same region (low lands, mountainous regions). The example also shows that distance classes between 50 and 170 km are more heterogeneous recognizing its higher standard deviations. In order to minimise heterogeneity in these regions, a further subdivision is required in these parts of the catchment.

To ensure more homogeneous sub-basins an algorithm was developed based on consisting of:

1. An objective function which identifies the needs and (if necessary) the region of further subdivisions.
2. A tool to specify the subdivision points in the selected region for subdivision of the catchment.
3. An evaluation strategy to assess performed subdivisions.

The following subsections give a brief introduction to these three functionalities, before the sequence of the algorithm is described. More details on the introduced tools have been listed up in Appendix A.

3.2.1 Objective Function

As outlined before the standard deviation $\sigma(C)$ can be used as an indicator for the heterogeneity of the sub-areas. Looking at the results of the distance-factor function for σ(AWC) of the Mulde (Fig. 6) the $1\cdot\sigma(C)$-range clearly indicates regions with higher heterogeneity. These regions should be considered for subdivision. In order to build this into the GIS-based algorithm, a threshold value Ω was introduced that states whether a distance class is to categorise by (relatively) "low" or "high" standard deviations. The threshold Ω is derived from the data by:

$$\Omega = \frac{\sum_{i=1}^{N_S} \omega_i^e \cdot \sigma(C)_i}{\sum_{i=1}^{N_S} \omega_i^e}, \tag{4}$$

where N_S is the number of distance classes in the basin, the exponent e is the parameter of a (non-)linearity factor and ω is a weighting factor defined as:

$$\omega_i = \frac{\sigma(C)_i - \max_{1\le i\le N_S}\left(\sigma(C)_i\right)}{\min_{1\le i\le N_S}\left(\sigma(C)_i\right) - \max_{1\le i\le N_S}\left(\sigma(C)_i\right)}. \tag{5}$$

The actual objective function Z is the number of distance classes that display a standard deviation higher than the threshold Ω. It is defined as the cardinality of the set of distance classes fulfilling this condition:

$$Z = \left|\left[i \mid 0 \le i \le N_S; \sigma(C)_i > \Omega\right]\right| \rightarrow \min \tag{6}$$

The proposed algorithm tries to minimize this value. Coherent distance-classes above the threshold are considered as *regions* of high variance regarding the characteristic in focus requiring a further spatial subdivision. If the standard deviation in coherent distance-classes stays below the threshold, these regions will be marked as low variance regions.

As the index N_S in Eq. (3) indicates, the threshold Ω is calculated for the entire catchment and does not necessarily represent the true value of $\sigma(C)$ for homogeneous sub-basins. It just helps to distinguish regions of high and low variances. Therefore it is recommended to vary the value of the non-linearity factor e in a range of $[0; \infty]$, though values between 0 and 1 were found most applicable in our case studies. If e is set to zero Ω is equal to the average of $\sigma(C)$ in the basin. As e is increased Ω lowers. The choice of e is dependent on the intention of the purpose of partition. If a detailed subdivision is required to capture the majority of heterogeneity e should be set to value greater or equal to 1. Otherwise if only regions with a significantly higher heterogeneity are to be captured e is recommended to be set to 0. However, in the presented case studies e has been set to 0.5. To indicate the range of potential results Ω is shown in all distance-factor functions for values of e ~ 0., 0.5 and 1.0.

3.2.2 Subdivision tools

The functionality of the proposed tools will be shown for the synthetic catchment (Fig. 3) introduced in the previous sections (more details in Appendix A).The application of the objective function was expected to result in one of the listed three potential outcomes:

1. The standard deviations in all distance-classes stays below threshold Ω,
2. Only parts of the classes have values of $\sigma(C)$ smaller than Ω,
3. Standard deviations of all classes are larger than Ω.

The first listed outcome would indicate that no further subdivision is required. The second would indicate that parts of the flow path display nearly homogeneous characteristics. This case is shown in Fig. 7a. Hatched cells indicate the low variance region. Since this region is homogeneous it will not require any further handling and can be separated from the residual, more heterogeneous parts of the basin.

To do so a tool called *Detachment* has been developed. The tool will determine the ideal drainage points ensuring their watershed covering the maximum range of low variance regions. The identification of these separation points is done iteratively close to the transition from low variance to high variance region. In Fig. 7b the result of *Detachment* is shown for the introduced synthetic catchment. Black dots indicate the identified drainage points, hollow points indicate potential separation points which were rejected in the course of iterations. After applying the *Detachment* tool, three sub-basins are defined. One containing the low variance regions not requiring any further treatment and two sub-basins containing the remaining parts of the catchment.

Both remaining heterogeneous sub-basins, in this example, consist of distance classes with standard deviations above the threshold. This could be caused by different spatial patterns in the sub-areas. On one hand, parallel streams, or more specific neighbouring valleys with different vegetation, slope etc. could cause higher variance. On the other hand a zoning of

hillslopes and higher elevated parts of the basin framing the drainage network (e.g. gley horizons close to stream) could results in higher values of the standard deviations. Such patterns are a result of the co-evolutional formation of catchments (Blöschl et al., 2013; Sivapalan, 2005).

Further tools were developed specifically for these two different potential root causes for heterogeneity. The first tool will provide a subdivision at stream branches (because our perspective of analysis is directed upstream; downstream would mean confluences) which will define new sub-basins at branching points of higher order streams. The *pruning* tool identifies branches by distance-factor functions of flow accumulation (see Appendix A).

The second tool is a *zonal classification* scheme, designed to account for heterogeneity within a distance class that is not caused by neighbouring valleys. We classified three zone types with an individual extent determined iteratively subject to three variables, i.e. Strahler order, distance to stream (compare x_H Sec. 3.1) and heights. The first zone type "*close to stream*" will be determined by the Strahler order and is intended to cover the stream-network. Individual streams (beginning at the highest Strahler order and adding lower orders successively) and its extent (distance to the stream, beginning with $1 \cdot \Delta o$) close to stream zones are determined iteratively, as already mentioned. The second zone type, referred to as "*transition*" zones, is first defined as all cells of the sub-basins not "*close to stream*". Subsequently, these cells are reassigned by their height-value either into "*high elevation*"- (heights above the iterated threshold) or into "*transition*" (heights below threshold)-zones. The height threshold mentioned before is iteratively determined as the quantile of the histogram of height of all non-"*close to stream*" zones.

In Fig. 7d & e the results of an application of both tools for the exemplary synthetic catchment are shown. Hatched cells in the lower left area indicate high variance regions that require partition. The *pruning* resulted in two additional drainage points and split this region into three sub-basins. The *zonal classification* provided no new drainage points but specified three zones for the previously defined drainage points. Note that the algorithm has the potential to reject a zonal classification if the resulting variance is equal or higher than for the un-classed sub-basin. In this case all cells will be marked as "*None*" zones.

The introduced tool-names will be used in Sec. 3.3 (and Fig. 8) where a detailed description and explanation of the algorithms' sequence will be provided.

3.2.3 Evaluation scheme

After the application of each previously introduced tools it has to be evaluated if its target has been achieved, i.e. minimising heterogeneity through the introduction of sub-basin and zones. Since our assessment of heterogeneity was based on the evaluation of distance-classes, we could also define our objective as the minimisation of the standard deviation within each distance class. No matter which tool has been applied, in some or all distance classes of the original sub-basin U multiple sub-basin / zones are present afterwards. Since the standard deviation was calculated for each partition unit (sub-basin or zone) individually, we were able to calculate the average standard deviation of neighbouring units within a distance class. This evaluation technique can be described as follows:

- *B* specifies the number of the sub-basins defined within the original catchment U.
- As first step we estimated the standard deviation $\sigma(C)$ (Eq. 2) within each sub-basin within distance classes based on flow length to the outlet of this sub-basin.As second step the calculated $\sigma(C)$-values were transferred to the flow-length axis of the original watershed U.
- This was done for all sub-basins by adding the stream flow length between their points of confluence and the outlet of the basin.
- Finally, the new standard deviation $\sigma_S(C)$ for the separated basin was calculated for each distance class of U as average of $\sigma(C)$-values assigned to the class of the initial sub-basin (U).

$$\sigma_S(C)_i = \frac{1}{\sum_{p=1}^{P_i} w(i \cdot \Delta s)_p} \cdot \sum_{p=1}^{P_i} \sigma(C)_{i;p} \cdot w(i \cdot \Delta s)_p \ , \tag{7}$$

with P_i being the number of parallel basins or zones, $w(i \cdot \Delta s)_p$ the number of cells within the distance-class *i* of the considered parallel basin/zone *b* and $\sigma(C)_{i;p}$ being the neighbouring standard deviations. The success of the partition can be measured by comparison with the standard deviation of the unseparated basin $\sigma_U(C)$, e.g. as the quotient of these values. With the new value $\sigma_S(C)$ the effect of each subdivision can be measured independently from the objective function (and its threshold).

3.3 Sequence of the algorithm

The tools presented above are at this point incoherent. Their sequential application in the ACS-algorithm (**A**scertainment by **C**atchment **S**tructure) will be explained step-by-step following the sequence shown in the flowchart in Fig. 8. Our considerations leading to the presented sequence can be summarized as follows:

1. Homogeneous regions should be separated from the remaining basin by the algorithm.
2. Preferably a basin should be subdivided into sub-basins at major branches/confluences of the river network.
3. For high variance regions the two options *pruning* and *zonal classification* should be carried out simultaneously, since the origin of high variance is unknown.
4. The results of both techniques (*pruning* or *zonal classification*) should subsequently be compared with the subdivision yielding a lower $\sigma_S(C)$ to be saved (other results to be discarded)
5. *Zonal classification* to be additionally applied in cases where only low variance regions are present. Independent of the target to reduce $\sigma(C)$, this way all ascertained sub-basins would obtain a zonal classification.

At the very beginning of the sequence, on initialisation of the algorithm, we would consider just one drainage point, i.e. at the outlet of the basin. After calculation of its watershed and the determination of the width-function of accumulated partial areas it would be evaluated if we also needed to consider major branches (See Appendix for a detailed description of this procedure). Major branches would account for larger, main rivers within a catchment. Since large rivers consist of a large number of cells draining into them, branches/confluences of rivers are easy to be differentiated by size. If the test for major

branches would turn out to be true, the tool *pruning* is called to specify two new drainage points (sub-basin outlets). These would be saved and put on the schedule of the algorithm for later examination.

Should a subdivision occur, the algorithm would start again at the previously used point, this time only looking at the watershed between the previous and the newly defined drainage points. If no further major branch would be present, the algorithm would calculate the standard deviations of the characteristic of interest and the objective function to estimate the number of distance-classes above the threshold Ω.

There are three potential outcomes (see Sec. 3.2.2), i.e. Standard deviation in none, some, or all classes above threshold. For each outcome the algorithm had an option:

- If no standard deviation of a class is above Ω, no further partition would be required so that the analysis of this part of the basin was complete and subsequently the *zonal classification* would be started and its results were saved. The algorithm would then proceed and examine the next drainage point on its schedule.
- If only some classes are above Ω, a partition would be required but not in all areas. These areas would be clipped by the *detachment* tool. One or more new drainage points would be defined and added to the schedule. The algorithm would then start again at its last active point.
- In case that all classes were above threshold points 3 & 4 of our consideration would be started. Both tools would try to lower the heterogeneity assuming different root causes for variation. Results leading to a lower residual variance would be saved, other result would be discarded. The algorithm would then start again at its last active point.

This process would be repeated until all drainage points have been examined by the algorithm. The fact that each basin, or sub-basin, is analysed again after each subdivision, provides the opportunity to apply a pre-partition. This could be useful if an existing structure (like a gauging network) is analysed for further improvements or just for zonal classification.

4 Method analysis

In this section we will analyse the outcome of applying the proposed algorithm for our case study catchments. First, we will take a qualitative look at the ascertained sub-basins and zones to assess similarities between catchments and characteristics. Subsequently we will take a quantitative look at the performance of the algorithm relative to its intended function.

The ACS-algorithm has been applied to all four catchments for pore volume and surface slope. Ascertained sub-basins and zones are shown in Fig. 9 a-d (Mulde and Regen) and Fig. 10 a-d (Main and Salzach). Additionally, the distance-factor functions for standard deviation $\sigma(C)$ for the respective characteristic C, prior to and after partition of the catchment, are shown.

4.1 Qualitative Evaluation

Looking at the results it can be noted that the proposed zonal classification was applicable on almost all catchments. Just one sub-basin in the Mulde catchment rejected a zonal classification (Fig. 9a, red sub-basin). Additionally, the defined sub-basins for both characteristics (same catchment) are comparable and often identical. This is mostly caused by the subdivision at a major branch. Nevertheless, differences in the number and extent of defined sub-basins are visible. More important though are the similarities and dissimilarities of the defined zones.

Both applications within the Regen (Fig. 9 c, d) and Main (Fig.10 a, b) catchment resulted in similar patterns of "*high elevation*" zones. In the Main catchment even the extent of "*close to stream*" zones (CTS-zones) is very similar. Wide-spread CTS-zones do not seem to be necessary for pore volume in the Regen catchment. Looking more closely at the CTS-zones for pore volume and comparing them to the maps of pore volume (Fig. 2), we can see a pattern across all catchments. Especially in the Mulde and Salzach catchment very narrow CTS-zones have been defined for most parts of the basin. The occurrence of these narrow zones coincides with the presence of belts of different pore volumes around a major streams (best visible in the Mulde catchment, Fig. 2, middle region). The soil patterns are not visible in the Regen and play a minor role in the Main catchment, hence the distribution of CTS-zones is more likely to be extensive.

The same analysis for surface slope zones shows that these zones are in most cases, more extensive than the pore-volume zones and follow the valley structure of the DEM (Fig. 1). CTS-zones cover the streams and floodplains at the bottom the valleys, "*transition*" zones cover the hillslopes and "*high elevation*" zones cover higher located plains.

The interaction of zonal extent is best visible in the Salzach catchment which is the most diverse in all of its characteristics (very high mountains with high slopes, soils with high and nearly no storage capacity). A comparison of the outcome for pore volume and slope (Fig 9 c, d) with the respective maps (Fig. 1 & 2) shows that the "*high elevation*" zones for pore volume cover the bare soil and rock formations with nearly no pore volume and in case of slope application the higher elevated parts of the mountains with only little slope. "*Transition*" zones cover in this case the steep hillslopes between the (comparably) flat valley bottoms and high plateaus. In case of pore volume they capture the mid-range soils between the mountain top and the floodplains which are in both applications encompassed by CTS-zones.

From this analysis of spatial natural patterns and patterns in the ascertained sub-basins and zones we can draw the conclusion that the outcome of the ACS-algorithm is linked to the spatial organisation of the considered catchment.

4.2 Quantitative Evaluation

Having confirmed that the proposed algorithm can actually mirror the spatial organisation of the catchment, we will now evaluate if the heterogeneity of the specific characteristic has been decreased. As stated in Sec. 2.4 the intended function of the algorithm was the reduction of the number of distance-classes comprising a standard deviation $\sigma(C)$ above the threshold Ω (of the characteristic C). To evaluate the performance towards this target we will look at the reduction of $\sigma(C)$, defined as

the normalised sum of all *Ns* differences of the standard deviation of the unseparated catchment $\sigma_U(C)$ and the separated basin $\sigma_S(C)$:

$$\alpha_1 = \frac{\sum_{i=0}^{N_S} \left(\sigma_{U;i}(C) - \sigma_{S;i}(C) \right)}{\sum_{i=0}^{N_S} \sigma_{U;i}(C)}. \quad (8)$$

The standard deviation of the separated catchment $\sigma_S(C)$ is calculated according to Eq. 6. In addition to this we applied a second performance metric to evaluate to what extend our target has been met. The metric α_2 highlights cases where the total heterogeneity was decreased significantly, but still being above objective as defined by threshold Ω. The metric α_2 was calculated as the delta between threshold Ω and standard deviation in the separated catchment $\sigma_S(C)$, normalised by the delta between Ω and the standard deviation in the unseparated catchment $\sigma_U(C)$:

$$\alpha_2 = \frac{\sum_{i \in M(S)} \left(\Omega - \sigma_{S;i}(C) \right)}{\sum_{j \in M(U)} \left(\Omega - \sigma_{U;j}(C) \right)}. \quad (9)$$

In Eq. 8 *M* is the set of distance classes comprising a higher standard deviation than the threshold Ω:

$$\mathrm{M} = [\mathrm{i} \mid 0 \le i \le N_S ; \sigma_i \ge \Omega]. \quad (10)$$

Performance data for all applications were listed in Tab. 1. Including the number of ascertained sub-basins (demonstrating modelling/calibration efforts).

As already indicated in the distance-factor functions of $\sigma(C)$ (Fig. 9 and 10) the performance of pore volume applications is in all cases (and both evaluation subjects) was superior to slope applications leading to a 2 to 6 times higher level of reduction (between 46 and 65% total reduction of variance). The remaining variance above the threshold ranged between 0.9% and 25% for pore volume applications. Compared to slope applications this was better between 8ppt (Regen) and 67ppt (Mulde). Although the reduction of variance for slope might be inferior, yet up to 25% of variance could be compensated by the ACS-partition of the basin.

Focussing on cases with insufficient variance reduction we were able to identify some limitations for the algorithm. First we will look at the slope application. The achieved reduction was generally low and the remaining variance was still high, but especially the outcome of the Mulde basin is inferior to all other (slope) applications.

The reason for this inferior performance might be the shape and arrangement of the catchment itself. In contrast to the other basins, the Mulde basin can be described as triangular. Several streams arise from the south of the basin and converge gradually heading to the north. Yielding nearly parallel situated sub-basins with the same spatial organisation of heights and slope. As it can be seen in the distance-factor function, the variance increases in upstream direction nearly continuously, is equally distributed and remains on a (comparably) low level (see ordinate-axis of distance-factor functions for remaining basins in Fig. 9 and 10). Contrary to that, the remaining catchments offer different spatial patterns. Here, headwater

catchments with higher elevations and slope lie within same distance classes with plain catchment parts, offering a higher variance and, hence, a better opportunity for subdivision.

Another inferior case is the pore volume application in the Salzach basin. The shape of the basin as well as the amount of variation (see Fig. 10) cannot be explained as previously. Figure 10 shows the map of the available water capacity (AWC) in the Salzach basin on a lower scale and the distance-factor function for standard deviation of AWC. On the map red boxes highlight spots within the basin displaying much higher AWC-values than its surrounding areas. These spots are also visible in the distance-factor function. For the separated basin (red line) the peaks are still visible after the separation, although the basic height of the line has been lowered. This observation can only be interpreted such that the occurrences of such soil enclosures are a limiting factor for the reduction of heterogeneity with the ACS-algorithm. It does not restrict its applicability, though.

4.3 Dependence on basin structure

In the previous section we concluded that the shape of Mulde basin in combination with the present surface slope values could have been the root cause for the noticed decrease of performance. Additionally, the arrangement of pore volume values in the Salzach catchment could also have led to a decrease of performance. These conclusion brought up a fundamental question: was it the value-range of the considered characteristics or the spatial arrangement/basin shape that caused the issue? In other words: if we could examine the same basin with another set of values, would the outcome, i.e. the number of sub-basins, zonal extent and the performance criteria change?

The problem is that no basin is like the other and even parts of the basin display different structures and shapes than the entire basin. Therefore, it is unlikely that there is only a single causal factor for the noticed performance decrease

To overcome this issue we performed what we called a “resampling experiment”. The intention was to examine the same basin shape and spatial arrangement with a different set of values (just like a time series analysis). Therefore a quantile-exchange of values has been performed.

Due to their similar size the basins of the Mulde and Salzach have been chosen for resampling. First we took the maps for AWC of both basins (Salzach Fig.1, Mulde not shown, but spatial organisation is analogue to TPV, range of value from 51 to 471 mm) and calculated an empirical distribution function for each basin. Subsequently, the AWC values were replaced with their respective empirical quantile level. Finally, the distribution functions were exchanged (Mulde to Salzach and vice versa) and the quantile levels were replaced with the exchanged distribution function quantiles. Results are shown in Fig. 12. We repeated this procedure with the DEMs as the source data for surface slope.

With this, we admit, slightly confusing resampling procedure we virtually relocated the Mulde basin in a steep alpine environment with diverse soils while the Salzach basin was equipped with mid-range mountainous heights and more homogeneous soil. That way we were able to assess the same basin shape and spatial arrangement with different (natural reasonable) range of parameter values.

The ACS-algorithm has been applied to the resampled values of pore volume and surface slope. Ascertained sub-basins, zones and distance-factor functions of the respective standard deviation are shown in Fig. 13, performance values are tabulated in Tab. 2. In case of the Mulde basin the outcome did not change significantly. Ascertained sub-basins (number and shape) as well as zonal extent were very similar to the original results, performance values were stable. It can be noted that the distance-factor function for σ(AWC) had a very different shape than in the original basin (Fig. 6).

Application to AWC in Salzach basin showed a significant change in performance. While the total reduction decreased, the remaining variance above the threshold was 20ppt lower than in the original basin. This is also visible in the distance-factor function of σ(AWC). Compared to Fig. 11it can also be noted that previous peaks close to the outlet and in the more distant parts of the basin disappeared. This result could be explained by the missing enclosures which have been transmitted as high values to the Mulde basin. Here, the allocation of the highest values is not organised in enclosures but in the upper-middle of the catchment (see Fig. 12) following a stream-orientated pattern. The peak of standard deviation is clearly visible in the distance-factor function of the unseparated resampled basin in Fig. 13, but the techniques of the ACS-algorithm are able to encompass this structure. Hence, the reduction of variance remained on the same level. We also experienced a change in performance for the slope. The exchange of heights values led to a lower range of slope values and a lower amount of heterogeneity. These patterns resulted in all other applications in inferior α_2 performances. Still, the geomorphologic structure of the basin remained unchanged and heterogeneity could be assessed by the algorithm (visible through unchanged total reduction).

In conclusion we can state that the actual spatial arrangement, or more specifically its spatial organisation, defines the outcome of the algorithm. Since this was our initial intention, this can be noted as a positive study outcome. On the down side we had to recognise that patterns (in this case soil patterns) that do not follow the co-evolutional structure of a basin (between soil and streams) (Blöschl et al., 2013) cannot be captured satisfactorily by the proposed algorithm. Furthermore, a spatially homogeneous variation structure of catchment characteristic, independent from its actual amount of variation, is also complicated to assess with the ACS-algorithm. However, we were able to demonstrate that the proposed algorithm works well for catchment characteristics that offer wide range patterns (like soil properties). (In the supplement to this article we substantiate this statement by applying the algorithm to hydraulic conductivity data, results are in accordance to results of pore volume)

5 Method application

In the previous sections we have shown how the algorithm works, what results it produces and what information about the basins we gained from its application. But we have not yet assessed how useful it is and what benefits it could provide. We will address this topic in the following two sub-sections. In comparison to a common subdivision, we will first evaluate its reduction of variance and second show its benefits for designing a hydrological rainfall-runoff model.

5.1 Comparison to gauging networks

The most common subdivision scheme is based on the available gauging network. On one hand this is due to calibration requirements and on the other hand it is the only source for a reasonable partition of the catchment. Obviously, existing gauging networks are a result of multiple considerations and requirements, e.g. of water management issues. In some parts of the basin it tends to be denser than required to catch the natural heterogeneity within a river basin, but other hydrological aspects (e.g. scale problems) might not be considered in the network design sufficiently.

Comparing sub-basins defined by hydrological networks by looking at the results of the ACS algorithm might show differences in the number of separation points. Such a comparison might help to provide advice to decision makers on where to locate new gauges for reducing variances. It could also provide information about the usefulness of the ACS algorithm. (Please keep in mind that for the decision maker the usefulness of the algorithm might be limited by the informational value of the specific catchment characteristic for runoff generation processes.)

Two benchmark subdivisions were established:

1. A subdivision based on the gauging network to be compared to the obtained ACS-basins (without zones).
2. A subdivision based on the gauging network with an additional zonal partition by land cover, based on the suggestions by Lindström et al. (1997), an additional third zone "Rock/Bare soil" has been introduced to account for alpine structures in the Salzach basin. This to be compared to the full outcome of ACS.

Gauging networks and defined land cover zones are shown on the left of Fig. 14. The distance-factor function of standard deviations for pore volume (centre of Fig. 14) and slope (right) are displayed in addition to the results of ACS-subdivisions. Performance data were summarized in Tab. 3.

Looking at the distance-factor function for pore volume it can be recognized that the red-line, representing ACS-results, is below the blue (rep. gauges) and the green (rep. gauges & land cover) line for nearly all distances, demonstrating the advantage of ACS. The ACS-advantage is also confirmed by the performances measures in Tab. 3. The total reduction α_1 (Eq. 8) exceeds the achieved values for gauges & land cover (bench-2) by a factor between 1.3 and 1.8. Furthermore the remaining variance above the threshold α_2 (Eq. 9) is lower by between 16ppt to 45ppt. Please note that this advantage was accomplished with a significantly smaller number of subdivisions. This makes us conclude that the proposed algorithm is a more effective tool to reduce the heterogeneity of pore volume data, or any catchment characteristic that has a similar spatial organisation (see Supplement).

Similar to Section 4, results for slope provided a different impression and quality. In the distance-factor functions (Fig. 14) we can see that all lines are on an equal level and show no clear advantage for any of the partition strategies. Looking at the performance results in Tab. 3, we can see that without zonal classification the gauging network has an advantage to ACS-results. Especially the sub-divisions in the Mulde basin are ineffective. However, with the introduction of zonal classification the performance values are at a more comparable level, withα_1 results ranging between 8% and 17 % (with exception of the Regen catchment). Results for remaining variance, however, are more different (22-77% ACS and 30-54% Bench-2) which

points out that the benchmark partition captures the heterogeneity of slope at least at some points of the basin better than the ACS.

This result is, again, caused by the fragmented nature of surface slope values. As we have shown before the gauging catchments in isolation will not capture the heterogeneity of surface slope and its performance is subject to a zonal classification that can be described as small scale distributed and fragmented.

5.2 Modelling application

Our model of choice is the HBV_{96}-model (Lindström et al., 1997), due to the fact that we already used its recommended catchment zonal classification scheme, its obvious ability to incorporate zones and, after all, due to its common usage.

The HBV_{96}-model is a semi-distributed conceptual model. Each sub-basin has one lower and upper ground water storage responsible for slow and fast runoff generation. On top of these storages an arbitrary number of zones can be placed. Each zone has an individual atmospheric-, interception-, snow- and soil water-routine. In the original concept four types of zones are possible: Field, Forest, Lake and Glaciers. The latter has not been used in this study so we excluded its description. Field and Forest zones are conceptually identical; their purpose is to provide different parameters for different land cover. Lake zones do not include any soil routines. All precipitation on these zones is handed directly into the lower ground water storage. Since the modelling application is meant to be short, please see (Lindström et al., 1997) for further information about the model.

Our application case was the Mulde catchment due to good data availability. Daily mean discharge, precipitation sums, temperature means and sums of potential evapotranspiration time series from 1951 to 2011 are available for 39 gauged sub-basins (discharge data available for 20-39 gauges, dependent on time window).

Two spatial model setups were employed for application, both are shown in Fig. 15. The left part of Fig. 15 shows the bench-2 partition we already used in the previous section, based on gauging network, heights and land cover. On the right part of Fig. 15 our proposed subdivision of the catchment, based on gauging network and pore volume, is shown. The gauging network has been used as a pre-partition of the basin and the ACS refined the sub-basin density and defined zones for all sub-basins. We chose pore volume as catchment characteristic. Its spatial organisation has been incorporated in the spatial setup of the model. Our decision was based on the fact that ACS worked better for pore volume than for slope and that information about storage capacities seemed to be more valuable for a conceptual (storage based) model.

Besides the incorporation into the model structure we were able to use information about the catchment characteristics in the calibration process. Each (ACS) sub-basin featured three zones, each having an individual average value for pore volume. Since we minimised the heterogeneity of the respective characteristic we were able to assume a uniform distribution of this value for the entire zone. Now, an automated calibration routine benefitted from these information and we were able to reasonably couple parameters of the zones by their respective average of the characteristic.

Say, each zone included a parameter called X. An algorithm, like the BOBYQA-algorithm employed in this study (Powell, 2009), offers in each iteration step a guess for this parameter $\dot{x}$. The parameter guess is then transformed to the zonal-

parameter by the zone characteristic $E_{Zone}(C)$ normalized by the average value of the entire basin $E(C)$ and a linear coupling parameter k_X:

$$X_{Zone} = \frac{E_{Zone}(C)}{E(C)} \cdot \mathrm{k_X} \cdot \dot{x} \tag{11}$$

Please note that the coupling parameter is subject to the calibration process itself and linked to a single parameter. In this study we coupled 6 zonal-parameters that are related to soil properties. This coupling-scheme (comparable to studies by Gharari et al., 2014) has been additionally applied to the benchmark. Here, $E(C)$ in Eq.10 is omitted and applied only to field zones, while forest zones use an unchanged $\dot{x}$. Since the coupling of the benchmark subdivision is not based on any process assumptions, we additionally applied a free parameterisation, where all parameters within each sub-basin and zone can be used for model fitting.

As already mentioned we performed calibration by the BOBYQA-algorithm (Powell, 2009), progressively from the headwaters towards the outlet of the basin. Both benchmark calibrations employ the same spatial setup with 38 sub-basins and an average of 30 zones per sub-basins. Due to the different parametrisation strategies a different but equally high number of parameters are subject to the calibration (see Tab. 4). The ACS-structure employs 44 sub-basins but only 3 zones (except two sub-basins having only one zone), giving 51 parameters per sub-basins. Compared to the benchmark calibrations this number is six to nine times lower. A high number of parameters is assumed to offer a model structure with a higher flexibility to match the observed data, though its higher complexity might lower its performance. To compare our proposed model structure with a benchmark at a similar number of parameters we added a third calibration strategy. The performed approach coupled all zonal parameters as described above. This lowered the amount of parameters per sub-basin to 45 for both model setups. As it can be seen in Tab. 4 the total amount of parameters in the benchmark partition is higher than in the new ACS-based partition.

After the calibration (time period 1995-2006) we evaluated the model's performance in three validation periods. Two in direct (temporal) neighbourhood to the calibration period and the last at the very beginning of the time series. Model performance has been calculated as the average Nash-Sutcliffe-Efficiency (NSE) (Nash and Sutcliffe, 1970) of all gauges and is tabulated in Tab. 5. Results show that ACS-parametrisations are superior in all cases. Its increase in performance ranges from 17-52% in comparison to the free-, 11-21% to the 6-parameter-coupled benchmark and 5-19% to the all-coupled parametrisation.

Beside this "lumped" evaluation we compared the performance of the models at each gauge in each period. A comparison of NSE for 6-parameter coupled model is shown in Fig. 16, for ACS and free-benchmark model in Fig. 17. Comparison for the all-coupled parametrisation is shown in Fig. 18. We can see that the individual performances led to the same conclusion as the lumped performance, though some results are better for benchmark models (both parametrisations). To be more precise, in case of 6-parameter coupled model 20 points (rep. a single gauge in one of the time periods) are below equivalency (rep. a

better performance of the benchmark model), in case of the free-benchmark model 12 and for the all-coupled benchmark 23 points. Representing 15%, 9% and 20% of the evaluated cases.

In conclusion we had to ask ourselves: What is the result of this modelling study? Obviously, we could improve the modelling performance. In accordance with findings in literature we could prove that additional information relevant to hydrological processes improve the model performance (Finger et al., 2015; Li et al., 2015) and, furthermore, we can confirm that the spatial organisation of catchment characteristics (in this case pore volume) is a relevant information. The latter conclusion is drawn from the fact that the ACS-model offers a similar (or superior) model performance to the coupled model although it included less model parameters.

6 Conclusions

The intention of this study was to assess the spatial organisation of catchments and their characteristics as well as to evaluate the benefit we can gain from this information for the use in conceptual, semi-distributed hydrological models. First, we proposed the distance-factor function to assess the interaction of an arbitrary catchment characteristic with the flow path. Graphical representations of this function are capable to visualize the heterogeneity of the considered characteristic visible. We further build an algorithm on this proposed function, mainly focusing on factor-functions of standard deviations, with the objective to reduce the heterogeneity of the respective catchment characteristic. The proposed ACS-algorithm utilises three different techniques to reduce the heterogeneity that were developed by looking at the main sources of heterogeneity visible in natural catchments. The outcome of the algorithm offers a spatial subdivision of the catchment, at a minimum of standard deviation of the respective characteristic.

After the introduction of these methods we performed an extensive test of the ACS-algorithm. First, we tested model functionality and its limits of application on four different basins. We evaluated the spatial patterns we obtained relative to visible spatial patterns in the basins. Furthermore we compared the reduction of variance for different characteristics and basins. Next, we evaluated the usefulness of the obtained results. On one hand we compared the variance reduction to a benchmark separation and on the other hand we merged our results to a semi-distributed hydrological model. The modelling study demonstrated the benefits we can generate from incorporating the spatial organisation of the basin.

We were able to confirm that the distance-factor function is a useful tool to detect non-random spatial patterns and the interaction of catchment characteristics with the flow path. Furthermore we could confirm its capability to detect anomalies in the structure of the catchment, e.g. spots of different soil types that do not follow the co-evolutional structure of the basin.

The proposed ACS-algorithm provided satisfactory results for different catchment forms, sizes and patterns. Heterogeneity of characteristics with spatial patterns (like soils) turned out to be beneficial for the application of ACS algorithm in terms of variance reduction. For more fragmented characteristics (like surface slope) displaying a small-scale but spatially equally distributed heterogeneity the algorithm will certainly provide a subdivision and zonal classification, but the variance reduction was at a comparable level to common approaches for basin subdivision. In addition we identified the general basin

shape to be influential for the efficiency of the algorithm. Although this is quite obvious, we learned that basins arranged along a single axis (like a strict south to north orientation), with variance of catchment characteristics is highly correlating to the distance to the outlet, are more difficult to assess for the proposed algorithm.

Our future work will focus on two topics: On one hand we have to further improve the subdivision algorithm. At this point we are able to assess the structure of a single characteristic, while it is highly desirable to consider multiple characteristics. Additionally we will have to develop methods to encompass soil enclosures and fragmented characteristics. The latter problem might lead to the well-known HRU-concept. We have to study if such development is desirable. On the other hand we will address the value for catchment similarity studies. Following intentions by Mesa and Mifflin (1986), who suggested the width-function as an indicator for catchment similarity, it might be worthwhile to investigate how results of the distance-factor function can be used to characterise similarity.

7 Code & Data availability

Python code and Toolboxes for common GIS-Software products of the proposed ACS-algorithm are available at https://github.com/HenningOp/ACS. Spatial data used in this study (DEM, Soil data, drainage points) are made available as well.

Appendix A

In this Appendix details to the proposed ACS-tools are given for further understanding of the algorithm. Each tool will be addressed separately.

Detachment tool for low variance regions

Regions of small variance have no need for further subdivisions, hence they are detached from the rest of the basin. Since the exact allocation of these regions is known, all cells within can be defined as target area T (hatched in Fig. 7a). Remaining cells are drawn together as non-target area NT. If one random point of the basin is selected as possible separation point (SP) and its watershed is calculated, the set of points belonging to the watershed, or sub-basin, of SP, BSP is obtained. The calculated watershed BSP covers parts of T and NT and hence a coverage rate can be calculated as the proportion of the cardinalities of the intersections and their respective superset:

$$O_{SP} = \frac{\left|B_{SP} \cap T\right|}{\left|T\right|} - \frac{\left|B_{SP} \cap NT\right|}{\left|NT\right|}, \quad \text{(A1)}$$

which shall be maximised.

The objective of a detachment O is to find a separation point (SP) whose basin BSP covers a maximum of T and a minimum of NT. Please note that for regions located at the outlet of the basin or at its upstream boundary only one SP will be defined. Possible SPs are assumed to be allocated at the transit of the main stream from T to NT, or vice versa. An iterative search returns the coverage values O and the highest value is selected as SP, defining a new sub-basin. In the upper part of Fig. 7a the obtained separation as well as the rejected SPs of the iteration (hollow points) are shown.

Pruning at confluences/branches

To identify branches, the distance-factor function of flow accumulation (i.e. the cumulative number of cells draining into a cell) (FAcc) is examined. FAcc indicates the contributing drainage area to each stream cell. Hence, discontinuities in the distance-factor function indicate confluences of streams (See Fig. A2 for example of distance-factor function).

Beginning at the outlet (zero on the x-axis) two features are visible: a slowly decreasing line of high FAcc values, representing the main stream at the outlet, and a noise-like smaller range of FAcc values close to the abscise, caused by the smaller tributary streams and contributing areas. To identify major tributaries, this noise has to be removed. We assume that in the first distance class the disparity between main rivers and contributing hillslopes is most distinct. Within the first class a k-Means cluster analysis is carried out to divide high and low FAcc values. The threshold value τ_S is determined as:

$$\tau_S = \min_{c}\left[\max_{c1}\left[FAcc\right]; \max_{c2}\left[FAcc\right]\right] \cdot \left(1 - \frac{\gamma}{10}\right), \quad \text{(A3)}$$

where c_1 and c_2 indicate the clusters and γ is the reduction order and by default 0. The algorithm will start with the default value for γ and searches for the first branch in upstream direction. If no branch is found, the order γ is increased by 1. The maximum order is set to 10. Please note that the higher γ is set, the lower the threshold gets and more FAcc-values remain for analysis. The routine identifies the coordinates of the branch inducing the drop in FAcc values (see Fig. A2, for example at distance ≈ 80 km).

Drainage points of major streams or major stream branches are identified likewise. Before the objective function is called, prevailing FAcc values in the basin are checked. If the FAcc value of the tributary stream is higher than the threshold value τ_R, a subdivision is performed. This parameter is calculated as percentage of the maximum FAcc value in the entire watershed (e.g. 5%) once at the initialisation of the algorithm.

Zonal classification

The iterative search for the optimal zonal classification involves three parameter: reduction of Strahler order s_R, distance from stream *o* and heights quantile *h*. The maximum Strahler order within the considered sub-basin *mS* is also involved but it is a constant. Initial values are: $s_R = 0$, o = 0 and $h = 0/h_{ite}$ (note that h_{ite} is a required, user defined parameter > 1.). In each iteration step one of the three parameters is increased to its maximum value ($s_{R;Max} = mS$; $o_{Max} = 5$; $h_{Max} = h_{ite}$) creating a different composition of zonal extent.

s_R: Controls which cells within the basin are potential "*close to stream*" (CTS) zones. All stream cells of Strahler order greater/equal to mS-s_R and all non-stream cells draining into a stream cell fulfilling this requirement are potential CTS-zones.

o: Defines the width of CTS-zones. All potential CTS-cells with $x_H \leq o \cdot \Delta o$ (as defined in Sec. 3) are confirmed as CTS-cells, all remaining cells of the sub-basin are "*transition*" (TS)-cells.

h: Controls the threshold used to define "*high elevation*" (HE) zones. An empirical distribution function of heights (taken from the input DEM) of all FFS-cells is calculated. The height threshold τ_H is then calculated as the $h/h_{ite} \cdot 100$ [%] quantile of the empirical distribution function. All cells with an assigned heights > τ_H are filed HE-zones, all remaining cells are confirmed as TS-cells.

After each iteration the average, distance-based standard deviation (Eq. 6) is calculated. The parameter combination giving the lowest $\sigma_S(C)$ is chosen as result.

References

Band, L. E.: Topographic Partition of Watersheds with Digital Elevation Models, Water Resour. Res., 22, 15–24, doi:10.1029/WR022i001p00015, 1986.

Beven, K. J. and Kirkby, M. J.: A physically based, variable contributing area model of basin hydrology / Un modèle à base physique de zone d'appel variable de l'hydrologie du bassin versant, Hydrological Sciences Bulletin, 24, 43–69, doi:10.1080/02626667909491834, 1979.

Blöschl, G., Sivapalan, M., Wagener, T., Viglione, A., and Savenije, H.: Runoff Prediction in Ungauged Basins: Synthesis across Processes, Places and Scales, Cambridge University Press, Cambridge, 492 pp., 2013.

Bossard, M., Feranec, J., and Otahel, J.: CORINE land cover technical guide: Addendum 2000, EEA, Copenhagen, 2000.

Bremicker, M.: Das Wasserhaushaltsmodell LARSIM: Modellgrundlagen und Anwendungsbeispiele, Hochwasserzentralen LUBW, BLfU, LfU RP, HLNUG, BAFU, 2016.

D'Odorico, P. and Rigon, R.: Hillslope and channel contributions to the hydrologic response, Water Resour. Res., 39, n/a-n/a, doi:10.1029/2002WR001708, 2003.

Dunn, S. M. and Lilly, A.: Investigating the relationship between a soils classification and the spatial parameters of a conceptual catchment-scale hydrological model, Journal of Hydrology, 252, 157–173, doi:10.1016/S0022-1694(01)00462-0, 2001.

Finger, D., Vis, M., Huss, M., and Seibert, J.: The value of multiple data set calibration versus model complexity for improving the performance of hydrological models in mountain catchments, Water Resour. Res., 51, 1939–1958, doi:10.1002/2014WR015712, 2015.

Gharari, S., Hrachowitz, M., Fenicia, F., and Savenije, H. H. G.: Hydrological landscape classification: investigating the performance of HAND based landscape classifications in a central European meso-scale catchment, Hydrol. Earth Syst. Sci., 15, 3275–3291, doi:10.5194/hess-15-3275-2011, 2011.

Gharari, S., Shafiei, M., Hrachowitz, M., Kumar, R., Fenicia, F., Gupta, H. V., and Savenije, H. H. G.: A constraint-based search algorithm for parameter identification of environmental models, Hydrol. Earth Syst. Sci., 18, 4861–4870, doi:10.5194/hess-18-4861-2014, 2014.

Grayson, R. and Blöschl, G. (Eds.): Spatial patterns in catchment hydrology: Observations and modelling, Cambridge Univ. Press, Cambridge, 404 pp., 2001.

Gupta, V. K. and Mesa, O. J.: Runoff generation and hydrologic response via channel network geomorphology — Recent progress and open problems, Journal of Hydrology, 102, 3–28, doi:10.1016/0022-1694(88)90089-3, 1988.

Gupta, V. K., Waymire, E., and Wang, C. T.: A representation of an instantaneous unit hydrograph from geomorphology, Water Resour. Res., 16, 855–862, doi:10.1029/WR016i005p00855, 1980.

Jenson, S. and Domingue, J.: Extracting topographic structure from digital elevation data for geographic information-system analysis, Photometric Engineering and Remote Sensing, 54, 1593–1600, 1988.

Kirkby, M. J.: Tests of the random network model, and its application to basin hydrology, Earth Surf. Process., 1, 197–212, doi:10.1002/esp.3290010302, 1976.

Lai, Z., Li, S., Lv, G., Pan, Z., and Fei, G.: Watershed delineation using hydrographic features and a DEM in plain river network region, Hydrol. Process., 30, 276–288, doi:10.1002/hyp.10612, 2016.

Li, H., Xu, C.-Y., and Beldring, S.: How much can we gain with increasing model complexity with the same model concepts?, Journal of Hydrology, 527, 858–871, doi:10.1016/j.jhydrol.2015.05.044, 2015.

Lindström, G., Johansson, B., Persson, M., Gardelin, M., and Bergström, S.: Development and test of the distributed HBV-96 hydrological model, Journal of Hydrology, 201, 272–288, doi:10.1016/S0022-1694(97)00041-3, 1997.

Mesa, O. J. and Mifflin, E. R.: On the relative role of Hillslope and Network Geometry in Hydrologic Response, in: Scale Problems in hydrology: runoff generation and basin response, Gupta, V. K. (Ed.), Scale Problems in hydrology, 2, Reidel, Dordrecht, 1–19, 1986.

Moore, I. D. and Grayson, R. B.: Terrain-based catchment partitioning and runoff prediction using vector elevation data, Water Resour. Res., 27, 1177–1191, doi:10.1029/91WR00090, 1991.

Müller, C., Hellebrand, H., Seeger, M., and Schobel, S.: Identification and regionalization of dominant runoff processes – a GIS-based and a statistical approach, Hydrol. Earth Syst. Sci., 13, 779–792, doi:10.5194/hess-13-779-2009, 2009.

Nash, J. E. and Sutcliffe, J. V.: River flow forecasting through conceptual models part I — A discussion of principles, Journal of Hydrology, 10, 282–290, doi:10.1016/0022-1694(70)90255-6, 1970.

Nobre, A., Cuartas, L., Hodnett, M., Rennó, C., Rodrigues, G., Silveira, A., Waterloo, M., and Saleska, S.: Height Above the Nearest Drainage – a hydrologically relevant new terrain model, Journal of Hydrology, 404, 13–29, doi:10.1016/j.jhydrol.2011.03.051, 2011.

Powell, M.: The BOBYQA algorithm for bound constrained optimization without derivates, Department of Applied Mathematics and Theoretical Physics, Cambridge, 2009.

Rigon, R., Bancheri, M., Formetta, G., and de Lavenne, A.: The geomorphological unit hydrograph from a historical-critical perspective, Earth Surf. Process. Landforms, 41, 27–37, doi:10.1002/esp.3855, 2016.

Rinaldo, A., Marani, A., and Rigon, R.: Geomorphological dispersion, Water Resour. Res., 27, 513–525, doi:10.1029/90WR02501, 1991.

Robinson, J. S., Sivapalan, M., and Snell, J. D.: On the relative roles of hillslope processes, channel routing, and network geomorphology in the hydrologic response of natural catchments, Water Resour. Res., 31, 3089–3101, doi:10.1029/95WR01948, 1995.

Rodríguez-Iturbe, I. and Valdés, J. B.: The geomorphologic structure of hydrologic response, Water Resour. Res., 15, 1409–1420, doi:10.1029/WR015i006p01409, 1979.

Schumann, A., Funke, R., and Schulz, G.: Application of a geographic information system for conceptual rainfall-runoff-modeling, Journal of Hydrology, 45–61, 2000.

Sivapalan, M.: Pattern, Process and Function: Elements of a Unified Theory of Hydrology at the Catchment Scale, in: Encyclopedia of hydrological sciences, Anderson, M. G. (Ed.), Wiley, Chichester, 193–219, 2005.

Snell, J. D. and Sivapalan, M.: On geomorphological dispersion in natural catchments and the geomorphological unit hydrograph, Water Resour. Res., 30, 2311–2323, doi:10.1029/94WR00537, 1994.

Soulsby, C., Tetzlaff, D., Rodgers, P., Dunn, S., and Waldron, S.: Runoff processes, stream water residence times and controlling landscape characteristics in a mesoscale catchment: An initial evaluation, Journal of Hydrology, 325, 197–221, doi:10.1016/j.jhydrol.2005.10.024, 2006.

Sponagel, H. (Ed.): Bodenkundliche Kartieranleitung: Mit 103 Tabellen und 31 Listen, 5., verb. und erw. Aufl, Schweizerbart, Stuttgart, 438 pp., 2005.

Verdin, K. and Verdin, J.: A topological system for delineation and codification of the Earth's river basins, Journal of Hydrology, 218, 1–12, doi:10.1016/S0022-1694(99)00011-6, 1999.

Vogt, J. V., Colombo, R., and Bertolo, F.: Deriving drainage networks and catchment boundaries: A new methodology combining digital elevation data and environmental characteristics, Geomorphology, 53, 281–298, doi:10.1016/S0169-555X(02)00319-7, 2003.

Table 1: Results of applications of *ACS*. Number of ascertained sub-basins, normalized reduction of standard deviation

	Pore volume			**Slope**		
Catchment	No. of Basins[-]	α_1 (Eq. 7) [%]	α_2 (Eq. 9) [%]	No. of Basins [-]	α_1 (Eq. 7) [%]	α_2 (Eq. 9) [%]
Mulde	38	54.3	10.4	30	8.2	77.9
Main	59	65.2	0.9	22	17.7	54.3
Regen	17	62.5	13.5	24	28.0	22.1
Salzach	24	48.5	25.6	38	15.1	56.0

Table 2: Normalized reduction of standard deviation for resampled basins

Catchment	**Pore Volume**		**Slope**	
	α_1 [%]	α_2 [%]	α_1 [%]	α_2 [%]
Mulde (res)	53.1	12.3	8.8	75.4
Salzach (res)	50.9	18.7	16.3	55.3

Table 3: Normalized reduction of standard deviation for sub-basins based on gauging network, ACS-basins and gauges and land cover

Catchment	**Pore volume**		**Slope**		**No. of Gauges**
	α_1 [%]	α_2 [%]	α_1 [%]	α_2 [%]	
Gauging network					
Mulde	24.2	53.4	9.4	69.9	40
Main	41.9	26.2	14.0	44.0	46
Regen	21.1	74.6	10.1	57.9	20
Salzach	30.3	48.8	9.6	68.5	33
ACS-basins only					
Mulde	32.8	45.3	0.0	100.0	38/30
Main	50.7	8.5	9.2	72.9	59/22
Regen	40.9	35.9	14.1	52.8	17/24
Salzach	40.6	24.6	9.3	73.6	24/38
Gauging network & land cover					**Occ. zones**
Mulde	35.3	35.0	14.5	54.8	2
Main	48.9	17.7	19.8	26.2	2
Regen	33.2	59.4	19.1	27.4	2
Salzach	38.4	50.1	21.6	30.8	3

Table 4: Parameter quantities

	Benchmark *Free*	Benchmark 6-*Coupled*	Benchmark *All coupled*	ACS 6-*Coupled*	ACS *All coupled*
Sub-basins	38	38	38	44	44
Zones per Sub.	~30	~30	~30	3	3
Parameter (total)	19562	12198	1710	2244	1980
Parameter (per Sub.)	~495	~321	45	51	45

Table 5: Nash-Sutcliffe Efficiencies of Benchmark and ACS-model

Simulation (Start-End)	$NSE_{B;Free}$ [-]	$NSE_{B;6}$ [-]	$NSE_{B;All}$ [-]	$NSE_{ACS;6}$ [-]	$NSE_{ACS;All}$ [-]
1995 - 2006 (C)	0.678	0.659	0.682	0.792	0.791
2007 - 2011 (V)	0.524	0.570	0.578	0.622	0.647
1984 - 1995 (V)	0.496	0.516	0.525	0.607	0.546
1951 - 1961 (V)	0.433	0.568	0.458	0.660	0.572

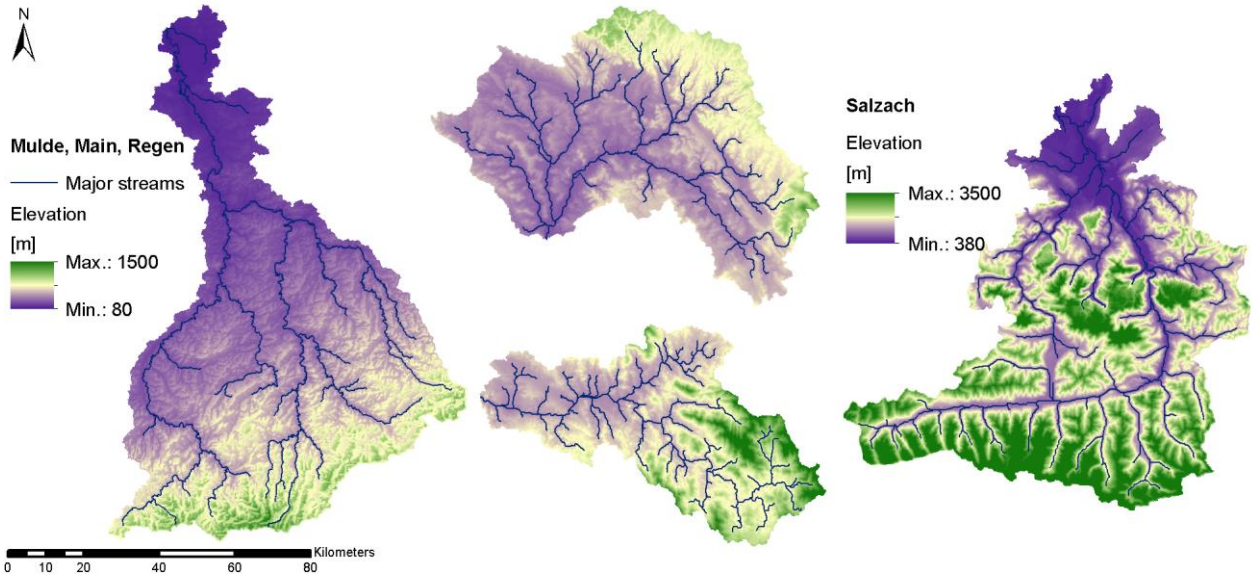

Figure 1: Digital Elevation models of the Mulde (left), upper Main (mid, upper case), Regen (mid, lower case) and the Salzach (right)

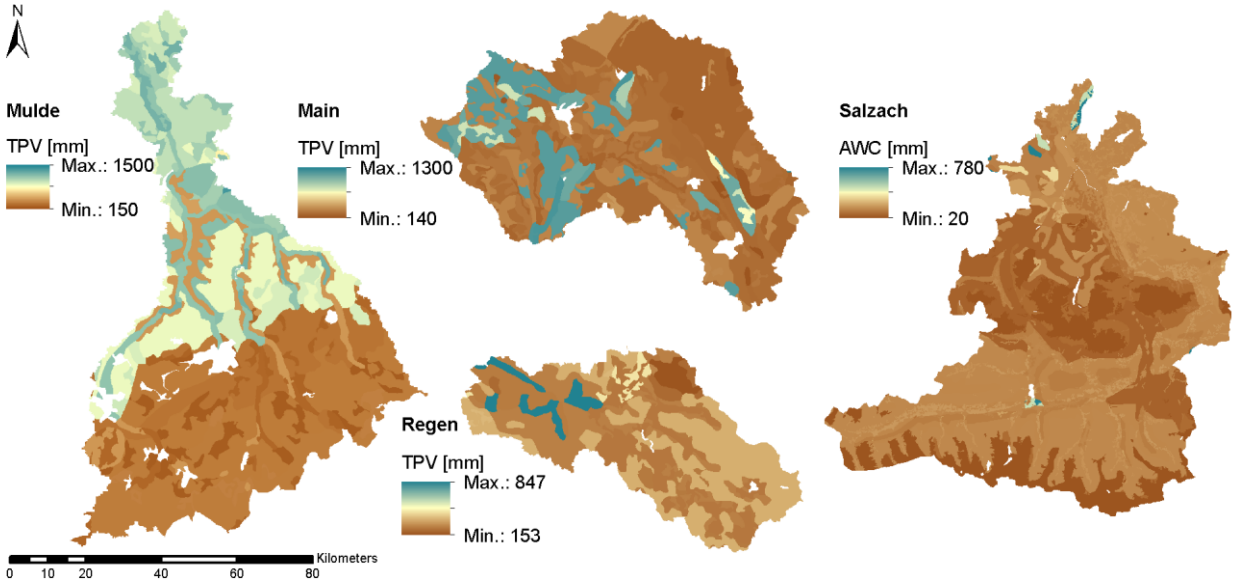

Figure 2: Values of total pore volume of the Mulde (left), upper Main (mid, upper case), Regen (mid, lower case) and AWC of the Salzach (right)

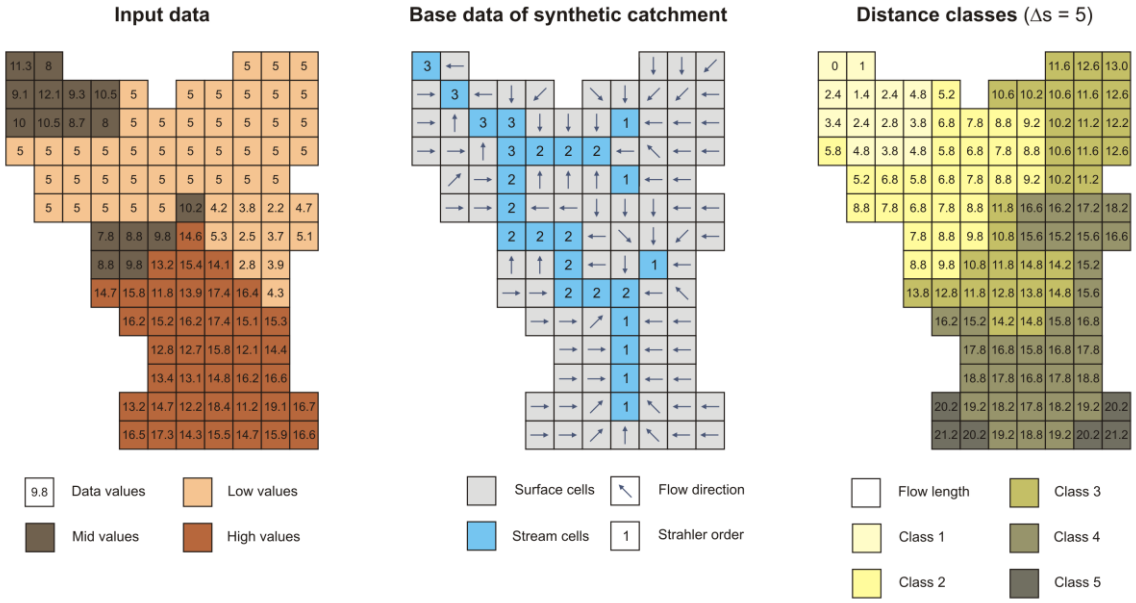

Figure 3: Exemplary input data (left), flow direction and Strahler order (middle) and distance data and –classes (right)

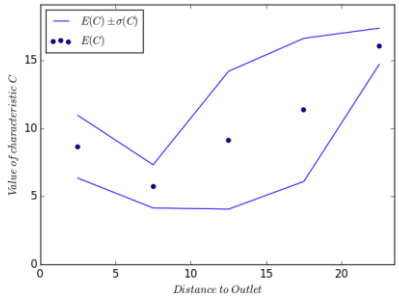

Figure 4: Distance-factor function of sample Data in synthetic catchment

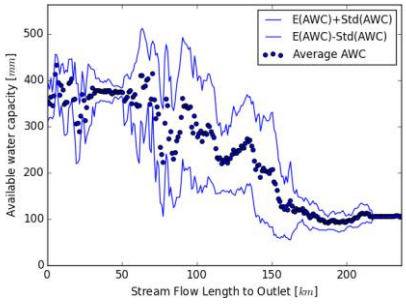

Figure 5: Distance-factor function of AWC in the Mulde catchment

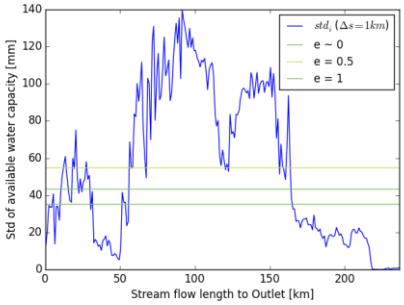

Figure 6: Distance-factor function of σ(AWC) and threshold values Ω for different values of e, in the Mulde catchment

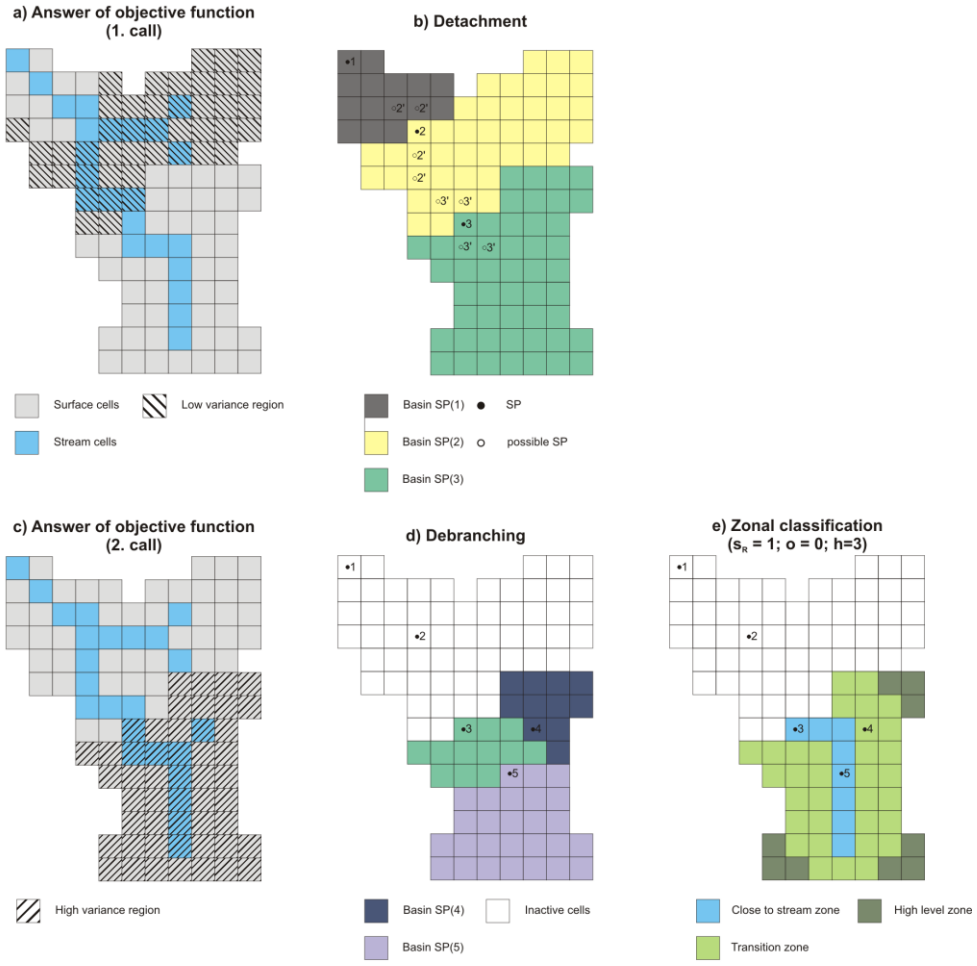

Figure 7: a&c) Answers of the objective function; result of b) Detachment, d) Pruning and e) zonal classification in the synthetic catchment

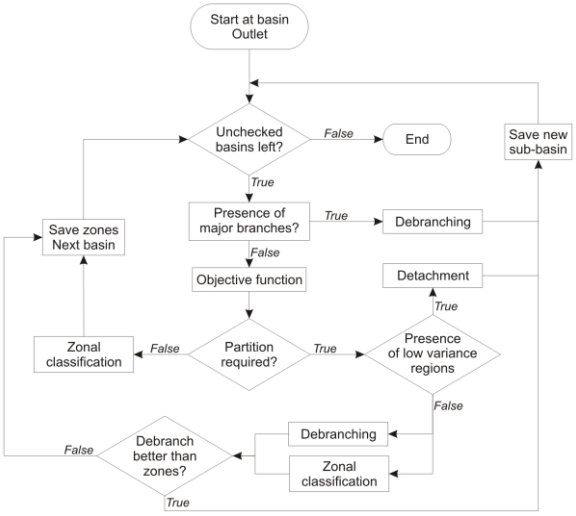

Figure 8: Sequence of the ACS-algorithm

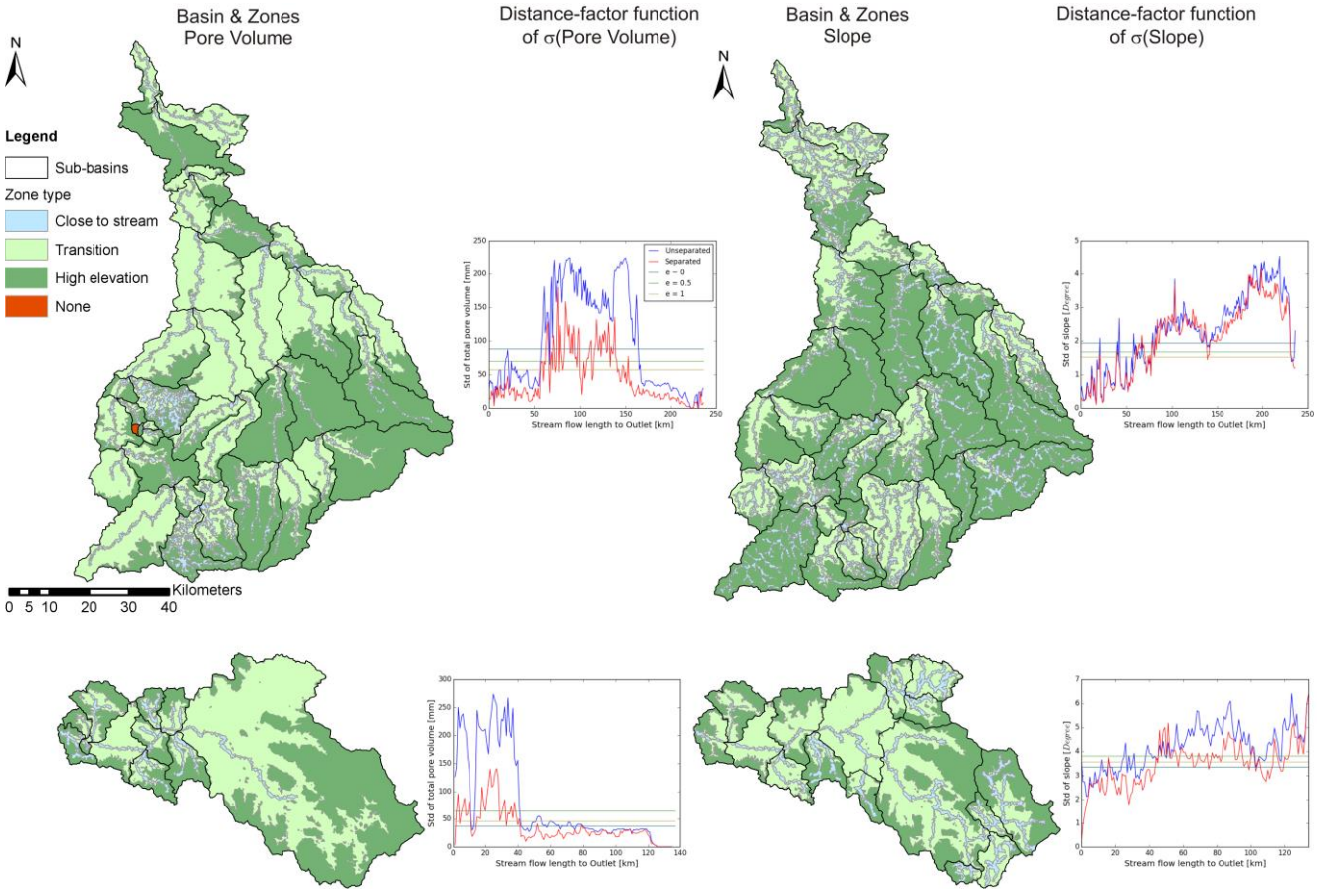

Figure 9: Results of ACS application for catchments of the Mulde and Regen, sub-basins based on pore volume (left) and slope (right). Comparison of $\sigma_U(C)$ and $\sigma_S(C)$ for each application (red and blue lines).

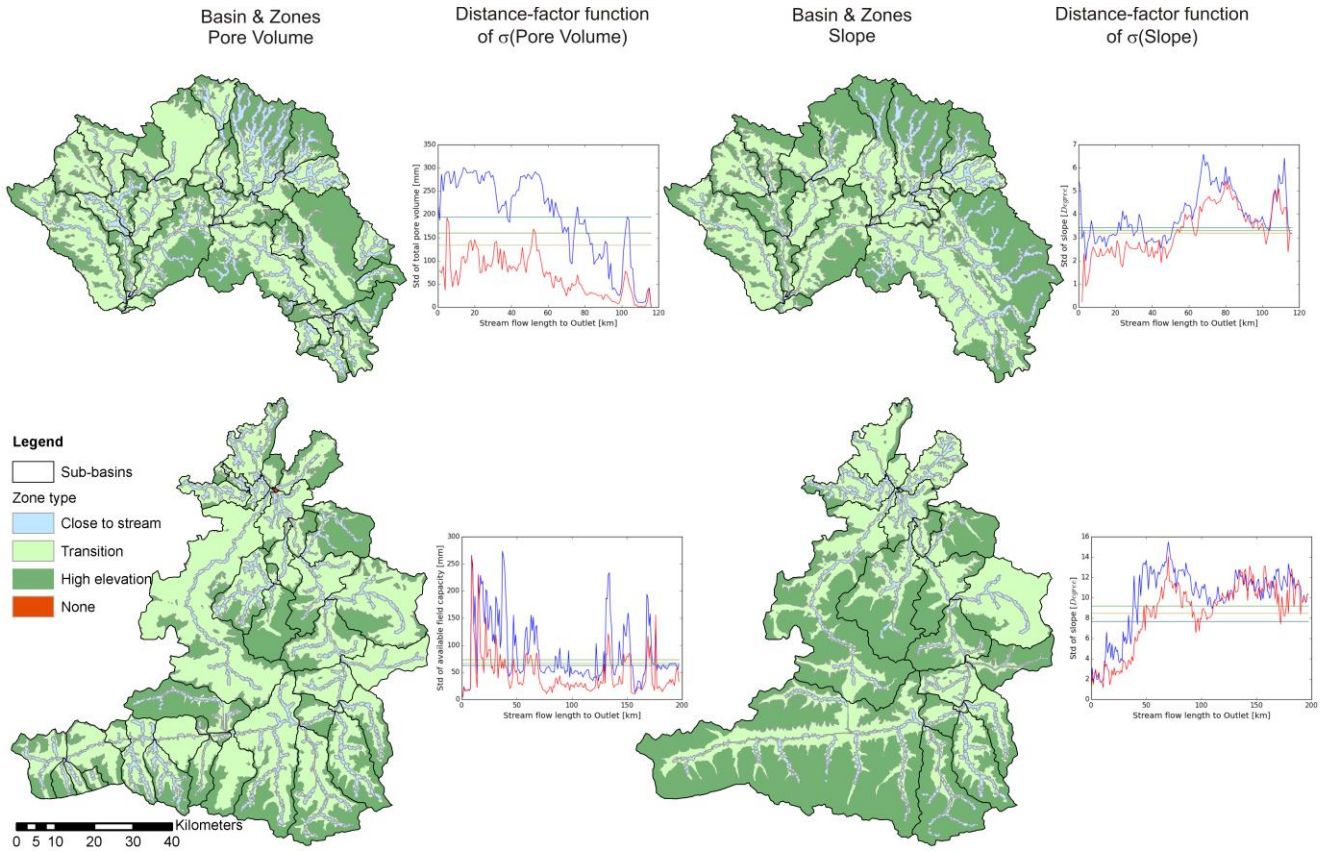

Figure 10: Results of ACS application for catchments of the Main and Salzach (from top to bottom), sub-basins based on pore volume (left) and slope (right). Comparison of $\sigma_U(C)$ and $\sigma_S(C)$ for each application (red and blue lines).

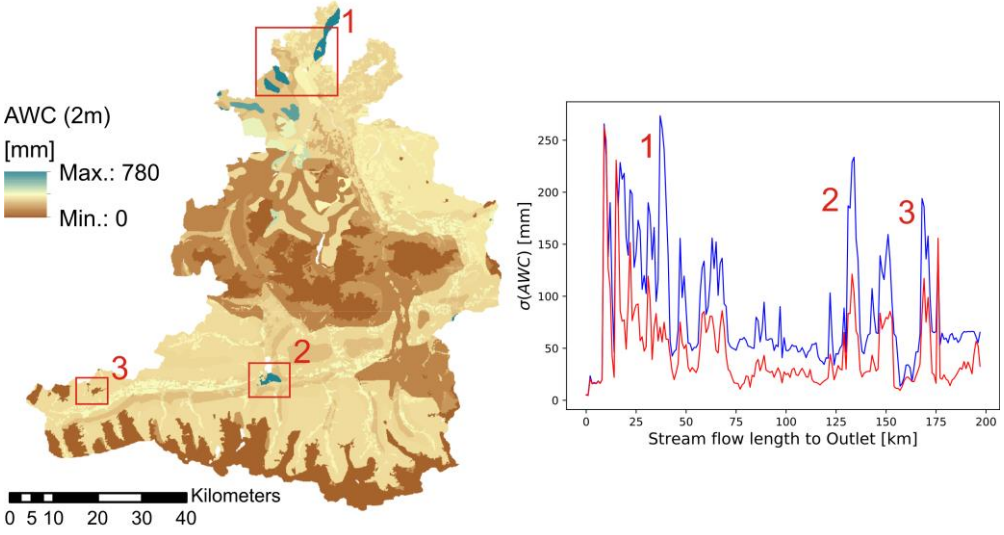

Figure 11: AWC of the Salzach catchment and the distance-factor function of $\sigma_U(C)$ and $\sigma_S(C)$. Red marked and numbered areas incorporating high value enclosures

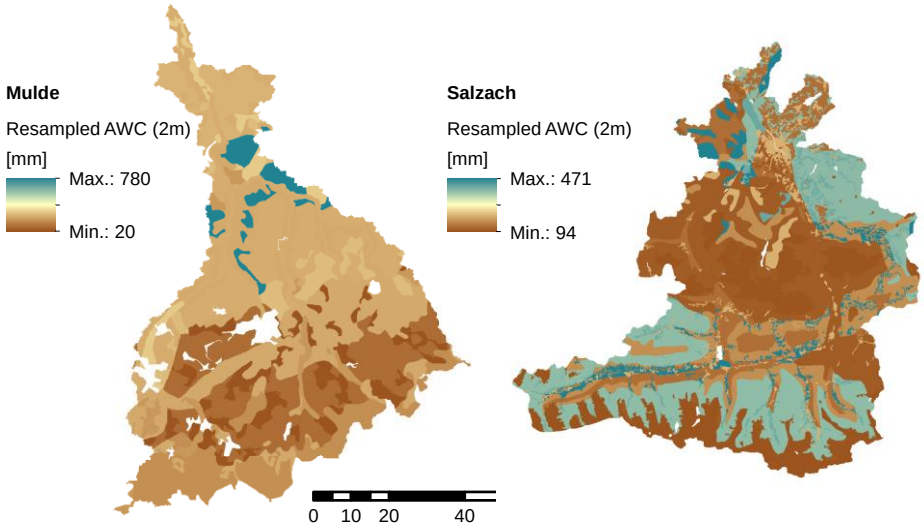

Figure 12: Resampled AWC values for Mulde and Salzach catchment

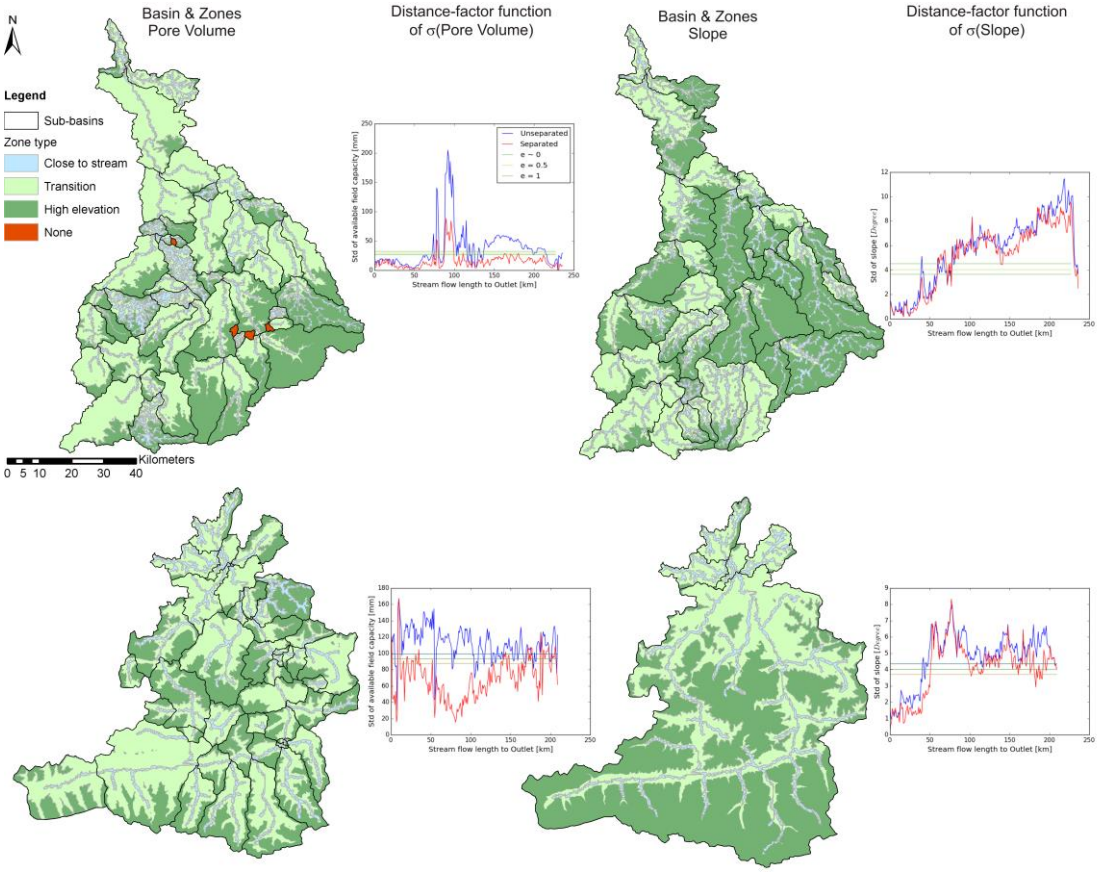

Figure 13: Results of ACS application for resampled catchments of the Mulde and Salzach (from top to bottom), sub-basins based on resampled pore volume (left) and slope (right). Comparison of $\sigma_U(C)$ and $\sigma_S(C)$ for each application (red and blue lines).

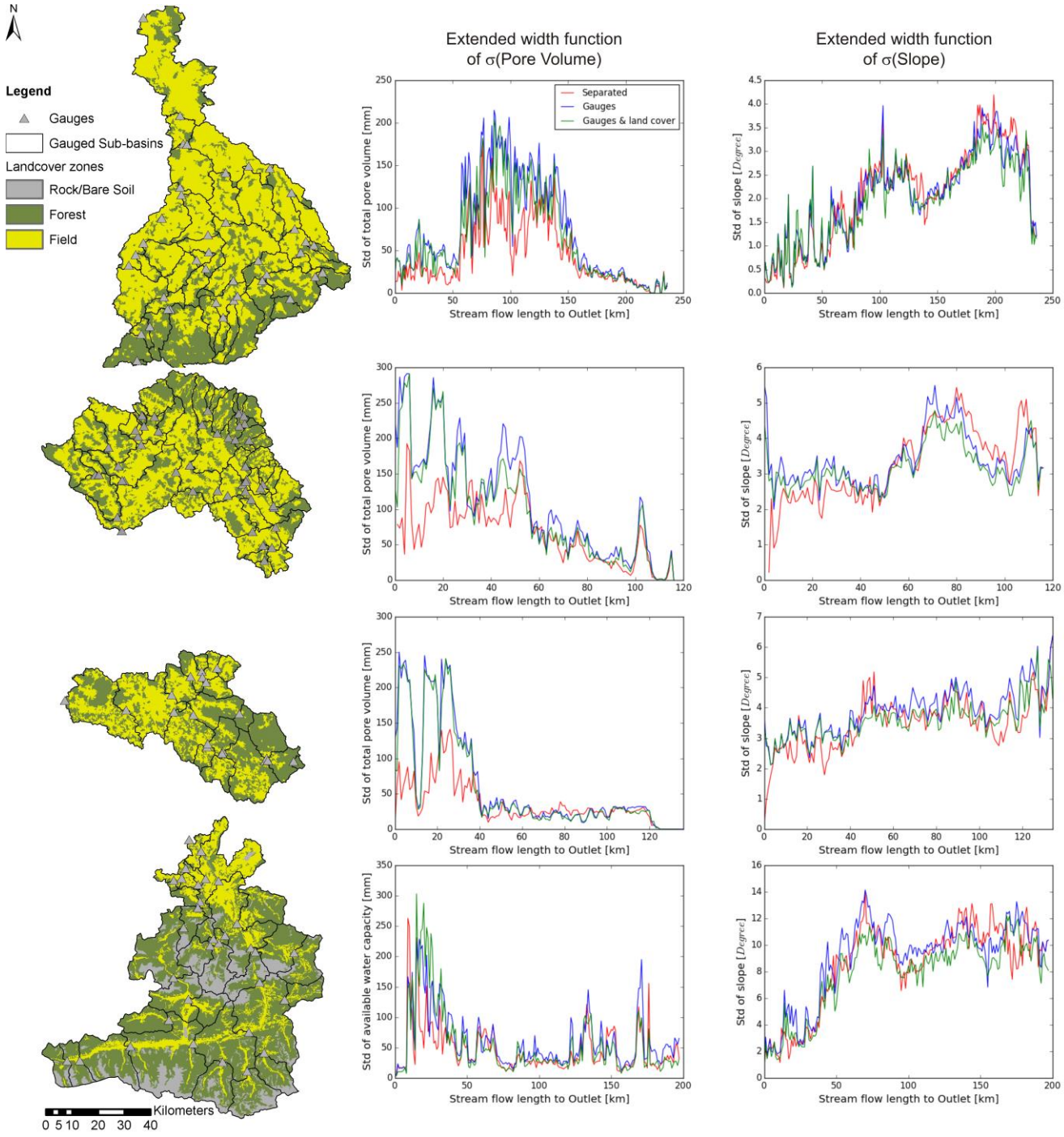

Figure 14: Subdivisions based on gauging network & zonal classification and distance-factor functions of *σ*(pore volume) and *σ*(slope) (left to right) for catchments of the Mulde, Main, Regen and Salzach (top to bottom)

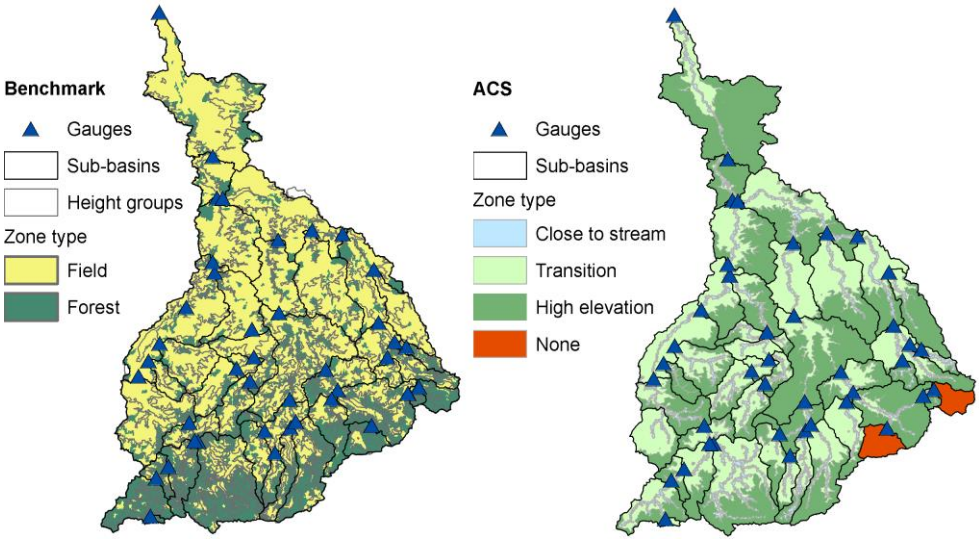

Figure 15: Spatial structures for HBV$_{96}$-Model: (left) ACS-basins & zones; (right) gauging network, land use & heights

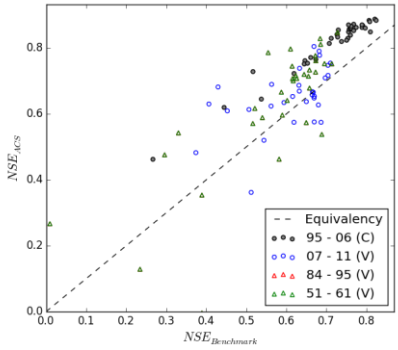

Figure 16: Nash-Sutcliffe Efficiency of ACS-based model and benchmark model, 6 coupled parameters

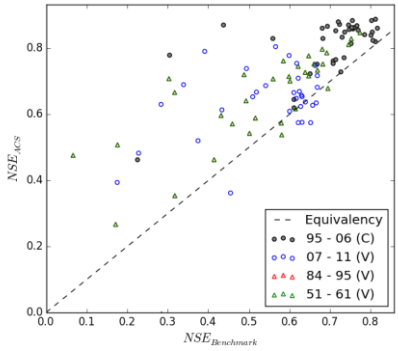

5

Figure 17: Nash-Sutcliffe Efficiency of ACS- based model and benchmark model, free parametrisation

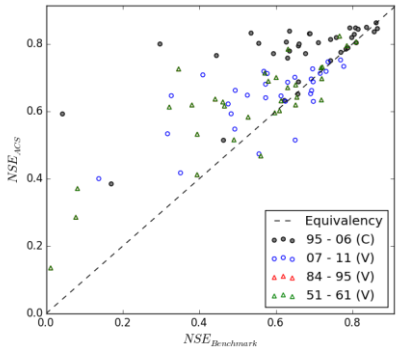

Figure 18: Nash-Sutcliffe Efficiency of ACS- based model and benchmark model, all zonal parameters coupled

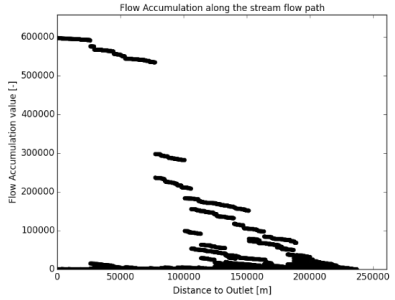

Figure A2: Distance-factor function of Flow Accumulation in the catchment of the Mulde